Title
A comparative study of molars and incisors in Beclin1 Knockout mice

Author
Kim, Soo Yeon Yeon

Publication Date
2021

Peer reviewed|Thesis/dissertation

UNIVERSITY OF CALIFORNIA

Los Angeles

A comparative study of molars and incisors in Beclin1 Knockout mice

A thesis submitted in partial satisfaction of the

requirements for the degree Master of Science

in Oral Biology

by

Soo Yeon Kim

2021

ABSTRACT OF THE THESIS

A comparative study of molars and incisors in Beclin1 KO mice

By

Soo Yeon Kim

Master of Science in Oral Biology

University of California, Los Angeles, 2021

Professor Reuben Kim, Chair

Mouse molars resemble human teeth, as their roots develop and stop growing. In contrast, mouse incisors grow and erupt continuously due to the presence of a persistent stem cell niche identified as the labial cervical loop, which actively gives rise to dentin-forming odontoblasts to support tooth homeostasis and injury repair. Autophagy (ATG), a cellular degradation process whereby macromolecules and organelles are sequestered to be recycled, has been shown to play a role in mineralized tissue-forming cells including odontoblasts. However, the precise role of ATG in odontoblasts *in vivo* remains unclear. Beclin1 is an indispensable ATG-related protein involved in ATG initiation. Therefore, we conditionally deleted Beclin1 in odontoblast-specific manner and generated $Becn1^{f/f}$;$Dmp1^{Cre/+}$ (Becn1 cKO) mice. From these mice, molars and incisors were evaluated radiographically and histologically. MicroCT scanning was employed to observe dentin formation and measure pulp tissue volume, histological analysis to examine dentin formation and dental pulp cells, and RNAscope *in situ hybridization* to identify odontoblast

differentiation in the incisor stem cell niche and mesenchymal tissue in molars. We further evaluated the *mRNA* expression of FGF signaling genes in human dental pulp stem cells *in vitro* using Becn1 knocked down dental pulp cells (DPCs). Becn1 cKO mice were born at the expected Mendalian ratio. However, Becn1 cKO mice at the 6th month mark exhibited increased obliteration of the pulp chamber in both molar and incisors. Interestingly, both Becn1 wildtype (WT) and Becn1 ckO mice a normal laCL histology. When Becn1 was knocked down in DPCs, Etv4, a downstream target gene of FGF signaling pathway, was significantly upregulated. Our study highlights the possible role of Beclin1 in pulp calcification of molars, as Beclin1 KO mice molars were characterized by a completely obliteration and calcification of the pulp space, and suggests that Beclin1 may play a role in developed teeth, but not in developing teeth.

The thesis of Soo Yeon Kim is approved.

Jimmy Hu

Bo Yu

Mo Kang

Reuben Kim, Committee Chair

University of California, Los Angeles

2021

TABLE OF CONTENTS

PAGES

Acknowledgements

I would like to express the deepest appreciation to my committee chair, **Dr. Reuben Kim**, for guiding me through the master's program and my journey in pursuing dentistry. His mentorship has been significant in my educational, professional, and career development.

I would like to thank **Dr. Sol Kim, Dr. Monica Yang**, **Dr. Wen Du**, and **Dr. Wei Chen** for working alongside me. They have helped me develop new skills in the lab and shared their expertise with me.

I would like to thank my committee members, **Dr. Jimmy Hu**, **Dr. Bo Yu**, and **Dr. Mo Kang** for all their time and support as I have been preparing my thesis.

I would like to thank UCLA and all the professors I've had who constantly challenged me to think critically.

Lastly, I would like to thank my family, friends, and God for their love and support as I pursued a Master of Science degree in Oral Biology.

1. Introduction

1.1 Beclin1 in bone homeostasis

Autophagy (ATG) is an essential cellular process that maintains cellular homeostasis and functions. ATG is a catabolic process whereby macromolecules and organelles are sequestered by vesicles and digested to be recycled. This pathway is characterized by the formation of double-membrane autophagic vesicles that fuse with lysosomes to generate single-membrane autolysosomes and followed by degradation of the encapsulated components. (Feng *et al*., 2013). ATG is best known for being activated upon nutrient starvation, as it supports cell survival under stressful conditions (Lee *et al*., 2014).

Beclin1, also identified as Atg6, is a highly conserved mammalian protein that belongs to the ATG-related family of proteins, which are key regulators in ATG. The mammalian gene encoding Beclin1 is similar in structure to the yeast ATG gene, atg6/vps30 (Kametaka *et al*., 1998), and is mono-allelically deleted in 40-75% of human breast cancers and ovarian cancers (Aita *et al*., 1999). Beclin1 plays a pivotal role in the initiation of phagophore formation by recruiting ATG-related proteins to the phagophore-assembly site (Boya *et al*., 2013, Xing *et al.*, 2012). Apoptosis and ATG are both regulated biological processes that play an essential role in tissue homeostasis, development, and disease. The mammalian anti-apoptotic protein, Bcl-2, interacts with Beclin1 to inhibit Beclin1-dependent ATG during nutrient-sufficient conditions in the context of yeast and mammalian cells (Pattingre *et al*., 2005). During cellular starvation, Bcl-2 is phosphorylated at residues T69, S70, and S87, which is followed by Bcl-2 dissociating from Beclin1. C-Jun N-terminal protein kinase 1 (JNK1), a stress-activated signaling molecule, regulates cellular starvation-induced Bcl-2 phosphorylation. JNK1-mediated Bcl-2 phosphorylation disrupts the Bcl2-Beclin-1 complex, leading to the activation of the class III

phosphatidylinositol-3-OH kinase VPS34-Beclin1 ATG complex. This pathway induces ATG. (Liang *et al*., 1999, Wei *et al*., 2008).

ATG has been shown to play an essential role in bone biology. Previously, we have reported that Beclin1 plays a fundamental role in osteoclasts (Arai *et al*., 2019). Beclin1 enhanced ATG and was required for osteoclast differentiation *in vitro.* Furthermore, osteoclast-specific inhibition of Beclin1 in adult mice exhibited an increase in cortical bone thickness caused by impaired osteoclastic function. These mice also were shown to have diminished trabecular bone mass, which was linked to a defect in cartilage formation and chondrocyte differentiation. This study identified Beclin1, an indispensable role in ATG, as a potential therapeutic target in bone-related diseases.

ATG has recently been addressed to have a role in mineralized tissue-forming odontoblasts by sustaining their longevity *in vitro* (Zhang *et al*., 2018, Couve *et al*., 2013). Progressive inhibition of ATG is reported to reduce the activity of odontoblasts and impair their capacity to perform dentin formation (Couve *et al*., 2013). Histone deacetylases (HDACs), a group of enzymes that remove acetyl groups from histone and non-histone proteins to regulate gene expression, has been reported to be involved in the differentiation process of bone-related cells. HDAC6, a unique member of the type II HDACs that localizes in the cytoplasm, has been reported to modulate the fusion of autophagosomes and lysosomes during odontoblast differentiation. When HDAC6 is not functional *in vitro*, autophagic-lysosomal fusion fails to occur. This caused a down-regulation of odontoblast differentiation in human dental pulp cells (Zhan *et al*., 2020).

In aged dental pulp cells, autophagy was increased (Lee *et al*., 2015). In addition, ATG marker (LC3) was detected within the odontoblast layer in human caries and pulpitis (Wang *et al.*, 2016)

In the context of inflammation, LPS stimulates odontoblast differentiation and associated with enhanced autophagy (Hui *et al*., 2017). Although there is growing evidence in literature that associates ATG with odontoblast differentiation, the role of Beclin1 and ATG in odontoblast differentiation *in vivo* still remains unclear.

1.2 Regenerative capacity of mice molars and incisors

Mice incisors grow and erupt continuously to compensate for functional attrition that constantly occurs at their incisal edges as they feed (Ohazama *et al.*, 2010). Interestingly, the regenerative capacity of mouse molars is limited; Mouse molars develop roots and stop growing. In contrast, mouse incisors continuously grow due to the presence of a persistent stem cell niche identified as the labial cervical loop (laCL). The laCL houses dental epithelial stem cells that drive the constantly growing mouse incisors (Yu *et al.*, 2020). A subpopulation of mesenchymal stem cells in the laCL continuously gives rise to transit-amplifying stem cells. These cells actively divide and give rise to pre-odontoblasts, terminally differentiated odontoblasts, and dental pulp cells to support tissue homeostasis and injury repair (KauKua *et al*., 2014).

Tooth mineralization starts with the secretion of dentin by odontoblasts, which are located at the periphery of the dental pulp. Upon tooth eruption, odontoblasts transition into a mature stage that maintains their capacity for secondary and reactionary dentin secretion. Pre-odontoblasts undergo cell growth, elongation, and polarization to become highly complex, mature secretory odontoblasts (Zhang *et al*., 2005). During odontoblast polarization, a mesenchymal cell undergoes morphological changes to transition into an asymmetrical odontoblast with a columnar cell body, which orderly aligns in a single layer along the dental pulp in the incisor stem cell niche. Cytoplasmic processes extend from the cell body to the pre-

dentin. The apical pole of odontoblasts is defined as the pole of odontoblast process which faces the dentin, and the basal pale faces the dental pulp (Ruch *et al*., 1995). The endoplasmic reticulum (ER), which functions in secreting extracellular matrix proteins, is found along the long axis of the cell and at a secretory vesicle rich rough ER-filled area. Odontoblasts have one main long process and multiple branches that protrude from the process at the apical role; The odontoblast processes function to secrete vesicles necessary for pre-dentin and dentin formation (Chang *et al.*, 2019).

The production of pre-dentin signals a shift in the patterns of synthesis from type III Collagen and fibronectin to type I Collagen and dentin phosphoproteins that comprises the dentin matrix. Once primary dentin is synthesized, secretory odontoblasts become smaller and less polarized transitional odontoblasts with reduced organelles and autophagic vesicles. ATG is important for rearranging organelles in odontoblasts as the cells transition from secretory to aged cells. Upon primary dentin formation, secondary dentin formation operates more gradually, continuing throughout the life of the tooth (Zhang *et al*., 2005).

Odontoblast markers, Dentin matrix protein 1 (DMP1) and dentin sialophosphoprotein (DSPP), are two non-collagenous proteins that belong to the small integrin-binding ligand N-linked glycoprotein family. Both proteins are abundantly present in the odontoblast to be secreted into dentin. During odontoblast differentiation, DMP1 binds to the D*spp* promoter to activate *Dspp* expression (Gibson *et al*., 2013). *Dspp* is expressed distal to the cervical loop, aligning with dentin (Narayanan *et al*., 2006). *Dspp* is differentially spliced to form dentin sialoprotein and dentin phosphoprotein, which are the major non-collagenous proteins (NCPs) of teeth that are secreted for dentin mineral deposition (Prasad *et al*., 2010). The histological appearance of dentin is derived from these NCPs.

1.3 FGF Signaling and its role in tooth development

The Fibroblast growth factor (FGF) family makes up one of the largest growth factor families. In vertebrates, this family of growth factors consists of 22 members that share 13-71% amino acid sequence homology in mammals (Ornitz *et al*., 2001). Twelve FGF family members are expressed in teeth and have been reported to play roles from the initiation of tooth development through tooth mineralization. FGFs bind to cell surface tyrosine kinase FGF receptors (FGFRs) (Ornitz *et al*., 2004). For the duration of tooth bud, cap, and bell development, FGF signaling is associated with tooth shape formation and differentiation of ameloblasts and odontoblasts. Additionally, this pathway is heavily associated with the homeostasis of the incisor stem cell niche. In the absence of Fgf10, ameloblast progenitor cells in the laCL led to reduced cell proliferation, whereas downregulation of Fgf3 caused a phenotype of reduced enamel mineralization and fragile incisors in mice. Mice lacking both Fgf3 and Fgf10 did not properly develop the incisor laCL (Li *et al*., 2014). Regarding the epithelial cells in the laCL, FGFs downregulate E-cadherin expression in the proximal region to permit cell migration from the stem cell niche, followed by proliferation and differentiation into ameloblasts (Li *et al*., 2012).

Furthermore, dysregulation of FGF signaling in FGF3, FGF10, FGFR1, FGFR2, and FGFR3 has been linked to congenital syndromes characterized by distinct morphological dental alterations. FGF3 and FGF10 bind to FGFR1-3, whose downstream effectors are BRAF/MEK/ERK and PI3K/AKT. FGFR1 and FGFR2 mutations have been identified patients diagnosed with Aper and Crouzon syndrome. These patients have hypodontia, most commonly on the third molar, maxillary lateral incisor, and mandibular second premolar. Missense

mutations in FGFR2, FGFR3, and FGF10 are linked to Lacrimo-auriculo-dento-digital (LADD) syndrome patients that have dental anomalies in tooth size and structure (Reitsma *et al*., 2014). Interestingly, Cinque *et al.* reported that JNK1-dependent activation of ATG initiation complex VPS34-Beclin1 is regulated by FGF18/FGFR4 interaction. *Fgfr4* homozygous and *Fgf18* heterozygous mutant mice failed to activate ATG and had decreased collagen levels in the growth plate. Treatment of synthetic Beclin1 peptide rescued the ATG level, collagen formation and femur length phenotypes in the mutant mice. This highlights FGF signaling as a fundamental regulator of chondrocyte ATG.

We hypothesize that Beclin1, the ATG-related protein, is associated with odontoblast differentiation and dentin formation. To test this hypothesis, we will generate mice with odontoblast-specific deletion of Beclin1 and observe the phenotypes in molars and incisors. MicroCT will be employed to observe dentin formation and measure pulp tissue volume, histological analysis to examine dentin formation and dental pulp cells, and RNAscope *in situ hybridization* to identify odontoblast differentiation in the incisor stem cell niche and molar mesenchymal tissue. Additionally, we hypothesize that Beclin1 is associated with odontoblast differentiation through FGF signaling. To test whether this is true, quantitative real-time PCR (qRT-PCR) will be utilized to measure the expression genes involved in FGF signaling in human dental pulp stem cells (hDPSCs). RNAscope *in situ hybridization* will be employed to examine the spatial expression of a transcription regulator downstream of FGF signaling.

Materials and Methods

2.1 Cells and cell culture

Primary human dental pulp stem cells (hDPSCs) were kindly provided by Dr. Songtao Shi (Herman Ostrow School of Dentistry, USC). Cells were cultured in α-MEM (Invitrogen) supplemented with 10% FBS (Invitrogen) and 5 μg/mL Gentamycin Sulfate (Gemini Bio-Products, West Sacramento, CA). To induce these cells to undergo differentiation and mineralization, cells (<5 passages) were cultured in the induction medium containing 10% FBS, 100 uM a 100 μM ascorbic acid 2-phosphate, 10 mM β-glycerophosphate, and 1.8 mM KH_2PO_4 (Sigma-Aldrich Inc., St. Louis, MO, USA) in α-MEM (Life Technologies).

2.2 Real-time quantitative RT-PCR

The cells were harvested with 1 mL Trizol reagent (Invitrogen) per sample. mRNA was extracted with High Pure RNA Isolation Kit (Roche Molecular Diagnostics, Branchburg, NJ, USA). cDNA was synthesized with PCR (SuperScript III Reverse Transcriptase; Invitrogen). Real-time PCR was done with SYBR Green I Master (LightCycler 480; Roche). A total of 45 cycles were executed, and the second derivative of the Cq value method was used to compare fold differences.

2.3 Alkaline Phosphatase (ALP) Staining/Activity and Alizarin Red S (ARS) Staining

ALP staining/activity was performed 7 d after induction using an ALP staining kit (86R-1KT; Sigma-Aldrich Inc.) according to the manufacturer's protocol. ARS staining was performed 3 wk after odontogenic induction. For ARS staining, cells were fixed with 1% formalin/phosphate buffered saline (PBS) for 10 min and stained with 2% ARS solution (pH of 4.1–4.3 with 10%

ammonium hydroxide) for 30 min at room temperature. The ARS solution was removed, and cells were washed with ddH_2O. The plates were photographed using both a microscope and camera. For the quantification of ARS staining, stained cells were destained in 10% acetylpyridinium chloride (Sigma-Aldrich Inc.) and measured at 562 nm using a microplate reader.

2.4 Generation of Beclin1 knockout mice

$Beclin1^{f/f}$ mice were obtained from Dr. Binfeng Lu (University of Pittsburgh School of Medicine), $DMP1^{Cre/+}$ mice from the Jackson Lab. These mice were crossbred to generate $Becn^{f/f}$;$DMP1^{Cre/+}$ mice. $Becn^{f/f}$;$DMP1^{+/+}$ (Beclin1 WT) mice and their littermates, $Becn^{f/f}$;$DMP1^{Cre/+}$ (Beclin1 cKO) mice were used in this study. The mice were maintained under specific pathogen-free conditions in the UCLA Division of Laboratory Animal Medicine (DLAM). All animal experiment protocols were approved (ARC protocol #2012-033 and #2011-062) and conducted according to the Animal Research Committee and the UCLA Institutional Animal Care and Use Committee.

2.5 Tissue Procurement

The mice maxilla and mandibles were carefully harvested and placed in a 50 mL centrifuge tube containing 4% paraformaldehyde in PBS, pH 7.4, at 4°C overnight to allow tissue fixation. The bone tissues were washed with 1X PBS followed by 70% ethanol storage.

2.6 MicroCT Scanning

The fixed mice maxillae and mandibles were wrapped in 70% ethanol-soaked gauze and placed in a 15 mL conical centrifuge tube for μCT analysis. They were subsequently scanned in SkyScan 1275 (Bruker Micro-CT, Kontich, Belgium) at a voxel size of 20 μm^3 and a 0.5-mm aluminum filter at 55 kVp and 145 μA, with an integration time of 200 milliseconds using a cylindrical tube (field of view/diameter, 20.48). Maxillary and mandibular tissues were reconstructed via the CTan and CTvol programs (Bruker microCT, Kontich, Belgium) to generate three-dimensional images and cross-sectional images. The pulp chamber images were generated by separating the pulp from the mineralized tissue on CTan.

2.7 Hematoxylin and Eosin staining

Upon completion of microCT scan, mouse maxillae and mandibles were decalcified using 10% EDTA. Becn WT and KO mice were decalcified for 3 weeks and 5 weeks, respectively. The decalcified maxillae were trimmed by making a sagittal cut immediately anterior to the first molar. The maxillae and mandibles were sent to University of California, Los Angeles Translational Procurement Core Laboratory and processed for paraffin embedding. Using the microtome, 5 μm thick sections of the formalin-fixed paraffin embedded (FFPE) tissues were prepared and mounted to Fisherbrand Superfrost Plus Microscope Slides. The precise areas of interest of the molars and incisors were established by examining the histology under the compound light microscope. The sectioned slides were deparaffinized at 60°C for 1 hour, followed by rehydration in ethanol with an increasing concentration of water. The rehydrated tissue slides were stained with hematoxylin for 2.5 minutes, washed with distilled water and 95% ethanol, and stained with eosin for 1 minute. The stained slides were dehydrated in 70%, 95%, and 100% ethanol, followed by xylene. The slides were mounted using mounting medium

Cytoseal™ 60 (Permount; Fisher Scientific, Houston, TX). Digital images were taken through an Olympus microscope (model DP72; Olympus Corp., Tokyo, Japan) at x100and X200 magnification.

2.8 RNAscope *in situ hybridization* (ISH)

FFPE sections were used for RNAscope ISH. RNAscope Multiplex Fluorescent v2 (Advanced Cell Diagnostics, 323110) was employed following the protocols of the manufacturer. The signal was detected by Opal™ 520 (Akoya Biosciences, FP1487001KT), Opal™ 570 (Akoya Biosciences, FP1488001KT), and Opal™ 690 (Akoya Biosciences, FP1497001KT). The probes used for this protocol were designed and synthesized by Advanced Cell Diagnostics. We substituted the target retrieval and protease steps with Pepsin Reagent, Ready to Use, Antigen Retriever, which had an incubation time of 30 minutes (Sigma Aldrich, R2283-15ML).

2. Results

3.1 Beclin1 knockout mice exhibit increased maxillary and mandibular bone thickness

To examine the role of Beclin1 in odontoblasts *in vivo*, we generated Beclin1 conditional KO (cKO) mice by crossbreeding Beclin1$^{f/f}$ mice with DMP1 $^{Cre/+}$ mice. When we crossbred Beclin1$^{f/f}$ and Dmp1$^{Cre/+}$ mice, Beclin1$^{f/f}$;Dmp1$^{Cre/+}$ (KO) mice were generated. These mice were small in size compared with their WT littermates, Beclin1$^{f/f}$;Dmp1$^{+/+}$ mice (Figure 1). The 6-month-old Beclin1 KO mice exhibited a narrow hard palate relative to Beclin1 WT mice (Figure 2). Sagittal cross sections of the maxilla demonstrated increased alveolar bone thickness in Beclin1 KO mice, which reflects the abnormal phenotype seen in the hard palate (Figure 3). Lingual and occlusal views of 6-month-old mice mandibles also demonstrated increased alveolar bone thickness (Figures 4 and 5). It is worth noting that the bone phenotype observed in Beclin1 KO around dentitions is not due to Dmp1-expressing odontoblasts. Although Beclin1$^{f/f}$;Dmp1$^{Cre/+}$ mice have Beclin1 deleted in odontoblasts, Dmp1 is also heavily expressed in osteocytes, result of which may explain the thickening of the alveolar bone. These data suggest that Beclin1 cKO mice exhibit an increased thickness of alveolar bone.

3.2 Comparison of molars and incisors in Beclin1 knockout mice

To evaluate whether Beclin1 deletion in DMP1-expressing cells affects odontoblasts, we investigated molars and incisors in the 2 and 6-month-old Beclin1 WT and cKO mice. uCT analysis revealed that both WT and cKO mice at the 2-month mark exhibited developed molars with normal pulp chambers. In sharp contrast, 6-month-old molars in Beclin1 cKO mice demonstrated a completely obliterated pulp space (Figures 6 and 7). When the pulp chamber volume was quantified, there was a notable reduction of about 50% in 6-month-old Beclin1 cKO

mice (Figure 7). When we investigated the incisors, we noted that the pulp chamber was phenotypically similar to the molars. Both genotypes demonstrated comparable incisor pulp chamber volumes at 2 months, whereas at 6 months, the Beclin1 cKO incisor pulp remarkably diminished (Figures 8-10).

To further investigate the role of Beclin1 in odontoblasts, we performed histological analysis of the molars and incisors. Consistent with the previous data, histological examination revealed that Beclin1 WT and cKO mice were born with molars that are of a similar size in pulp chamber. Strikingly, 6-month-old Beclin1 KO mice demonstrated completely calcified molars. These molars were noted by an absence of mesenchymal stem cells in the usual pulp space (Figure 11). In addition, histological analysis revealed that pulp calcification works from the dentin towards the inner region of the mesenchyme (Figure 12). This indicates that pulp calcification in the molar is due to tertiary dentin formation, which started as early as 2 months after birth, and Beclin1 may play a role in odontoblast-mediated pulp formation in molars of mature adult mice. When the incisors were evaluated, there was also an increase in dentin formation and reduced pulp space in odontoblast-specific Beclin1-deficient mice at the 6-month timepoint, similar to the phenotype seen in molars (Figures 13 and 14). It is interesting to note that Beclin1 KO mice began to form dentin more proximally relative to Beclin1 WT mice. Dentin formation of incisors began near the first molar in WT mice, whereas it began at the third molar in KO mice (Figure 9). These data suggest that Beclin1 plays a role in regulating dentin mineralization in both molars and incisors in mice.

To assess whether the enhanced dentin phenotype in Beclin1 KO mice were contributed by odontoblasts in the incisor stem cell niche, we further investigated the status of laCL. Histological examination revealed no visual distinction between the two genotypes, as normal

dentin formation and organized epithelium were demonstrated near the cervical loop of 6-month-old mice (Figure 15). In contrast to the mice molars, the incisor stem cell niche revealed no calcification at the proximal region of the laCL, which indicates a properly functioning proliferation and odontoblast differentiation site for dentin to be generated.

To investigate whether the incisor phenotype of Beclin1 KO mice was due to changes in odontoblast differentiation, we employed RNAscope *in situ hybridization* to examine the spatial expression of odontoblast differentiation marker *Dspp mRNA* in the laCL. In control mice, *Dspp* expression began proximally in the laCL, continuing across the pre-dentin, and colocalized with *Beclin1 mRNA* (Figures 16A-E). In the laCL of Beclin1 KO mice, *Dspp* expression was orderly aligned along the pre-dentin, resembling the phenotype seen in Beclin1 WT mice (Figures 16F-J). This data indicates that Beclin1 KO mice exhibited normal odontoblast differentiation in the laCL. When we investigated *Dspp* expression in mice molars, Beclin1 KO mice were revealed to have increased odontoblast differentiation across the dentin-pulp interface relative to control mice. Interestingly, some regions of the dental pulp began to dissipate, which was indicated by the presence of an additional DAPI-composed circle containing *Dspp* at the dentin-pulp border. (Figures 17E-H). This data suggests that Beclin1 may regulate odontoblast differentiation in the mesenchyme of mice molars.

3.3 Beclin1 expression may play a role in FGF signaling in the dental pulp

A previous study has demonstrated a critical role of FGF signaling in regulating bone growth and ATG in chondrocytes. Specifically, induction of ATG was shown to be mediated by the JNK1-dependent ATG initiation complex VPS34–Beclin-1 through growth factor FGF18 and FGFR4 interaction (Cinque *et al*., 2015). ETV4 is a downstream transcription factor in FGF

signaling that has been shown to be involved in proliferation and differentiation (Corral *et al*., 2017). Based on these reports, we decided to examine whether Beclin1 plays a role in FGF signaling in odontoblasts *in vitro.* We first examined whether Beclin1 is associated with mineralization in DPSCs. ALP and Alizarin Red staining were employed to identify odontoblast differentiation and calcium deposition, respectively. Our results reveal that siBeclin1-treated DPSCs exhibit enhanced odontoblast differentiation and mineralization upon induction with odontogenic induction medium (Figure 18 and 19), which indicates that Beclin1 may play a role in odontoblast-mediated dentin mineralization. We checked the relative mRNA expression levels of *Fgfr1, Ffgr2, Ffgr3, Ffgr4* and *Etv4* in siBeclin1-treated DPSCs, which give rise to odontoblast-like cells. *Fgfr1* was predominantly expressed in odontoblasts, whereas *Fgfr2, Fgfr3,* and *Fgfr4* were not expressed. Interestingly, *Etv4* expression significantly increased in odontoblasts upon Beclin1 deletion (Figure 20). This data indicates that Beclin1 may be associated with Etv4 through FGFR1 in odontoblasts *in vitro*. Future studies will be required to investigate whether Beclin1 regulates FGF signaling *in vivo*.

Discussion

In this comparative study of mice molars and incisors, we examine the role of Beclin1, an ATG initiator that forms the initial autophagosome complex (Sahani *et al*., 2014) and thereby an indispensable component of ATG, in $Becn1^{f/f}$;$Dmp1^{Cre/+}$ mice. Our study suggests that odontoblast-specific Beclin1 may regulate the dentin mineralization process in molars and incisors. In the absence of Beclin1, the pulp chamber volume reduces and dentin thickness increases in molars and incisors, highlighting the possible role of Beclin1 in odontoblast-mediated dentin formation (Figures 6-14). To further support these findings, future studies would include measuring the ratio of hard tissue to pulp in mice and quantifying the mineral density and dentin thickness, in order to quantify the pulp volume relative to tooth mineralization and confirm that we made proper visual interpretations of dentin thickness, respectively.

6-month-old mice with odontoblast-specific Beclin1 deletion have completely calcified molars, whereas 2-month-old mice displayed a normal pulp chamber. Although the latter are characterized by a normal mesenchyme, they begin to show slight calcification in the pulp space, indicating tertiary dentin formation. This data could be explained by the increased expression of the odontoblast differentiation marker *Dspp* seen in Beclin1 KO mice molars (Figures 17A-H), which also reveals moderate dissipation of the mesenchymal stem cells. In addition, histological examination reveals that pulp calcification works from the odontoblast layer towards the inner region of the molar mesenchyme (Figure 12). Based on this data, we expected the cells lining at the dentin-pulp interface to be a homogeneous population. Surprisingly, our RNAscope *in situ hybridization* data reveals that *Dspp* and *Beclin1 mRNA* are not continuously aligned across the odontoblast layer. This indicates the possibility of a heterogenous cell population found adjacent to dentin.

In 6-month-old Beclin1 KO mice, dentin mineralization was enhanced in the proximal region of the incisor. Therefore, we expected to see a cervical loop with normal epithelial organization, which would indicate a properly functioning incisor stem cell niche that gives rise to differentiated odontoblasts. If the laCL was disrupted by calcification, that may cause problems in proliferation, differentiation, and ultimately odontoblast-mediated dentin formation. The fully developed molars were characterized by a completely calcified pulp space, and incisors displayed increased dentin thickness that originated from a visually normal laCL. These data support that Beclin1 may play a role in teeth that have already developed, but not in developing teeth.

The laCL of Beclin1 WT mice revealed an orderly aligned *Dspp mRNA* expression across the pre-dentin (Figures 16A-E). *Dspp* was expressed not only where DAPI stains, but also outside it, reaching the pre-dentin layer (Figure 16E). *Dspp-Beclin1* colocalization occurred outside the DAPI staining (Figures 16A-E), which may suggest that Beclin1 associates with *Dspp* in the extended odontoblast processes, where tubular dentin formation occurs. Beclin1 KO mice revealed an orderly aligned *Dspp* expression across the pre-dentin (Figures 16F-J). Based on the enhanced incisor dentin thickness seen in Beclin1 KO mice (Figures 9, 13, and 14), we expected to see either a similar phenotype or a more proximal expression of *Dspp* relative to Beclin1 WT mice. Future studies would include measuring *Dspp* puncta to further support that there is no significant difference in odontoblast differentiation between the two genotypes. Interestingly, our results reveal a shorter length of *Dspp* expression in individual odontoblasts in the context of odontoblast-specific Beclin1 deletion. This suggests that Beclin1 may associate with the intracellular arrangement of *Dspp* in odontoblasts at the incisor stem cell niche. ATG has been reported to affect the secretion of proteins in different cell types. In some cell types, ATG

inhibition increases protein secretion. Specifically, immune cells enhance secretion of cytokines upon inhibition of ATG (Cotzomi-Ortega *et al*., 2018). Perhaps, ATG inhibition in odontoblasts may increase the secretion of the *Dspp* derivatives, DSP and DPP. Future experiments will be required to determine whether deletion of Beclin1, an indispensable component of ATG, induces NCP secretion for dentin formation.

FGF signaling has been linked to ATG through its receptors and growth factor ligands. Cinque *et al.* reported that FGF18/FGFR4 activates ATG through the ATG initiation complex VPS34-Beclin1. Our *in vitro* studies revealed that ETV4, a downstream effector of FGF signaling, significantly increased in siBeclin1-treated DPSCs. We expected to see a predominant expression of *Fgfr4* since *Etv4* expression increased. However, our data suggests that FGFR4 is not related to odontoblasts. Instead, FGFR1 is predominantly expressed, which indicates that this receptor may play a role in odontoblast differentiation. Previously, Krivanek *et al*. has reported that *Etv4* expression is induced during odontoblast differentiation. Therefore, the increased expression of *Etv4* seen in vitro may reflect the enhanced dentin formation phenotype seen in our mice model. Thus, future studies would require further investigation of the role of Etv4 in odontoblasts, and whether Etv4 is regulated by FGFR1 in vivo and in vitro.

Conclusion

This comparative study reveals that molars and incisors in Beclin1 WT and KO mice have similar histology and increases in calcification as they get older. Our study also highlights the possible role of Beclin1 in pulp calcification of molars, as Beclin1 KO mice molars were characterized by increased obliteration and calcification in the pulp space. Beclin1 may play role

in developed teeth, but not in developing teeth. Lastly, our in *vitro* data indicates that Beclin1 may associate with FGF signaling through *Etv4*.

Figures

1

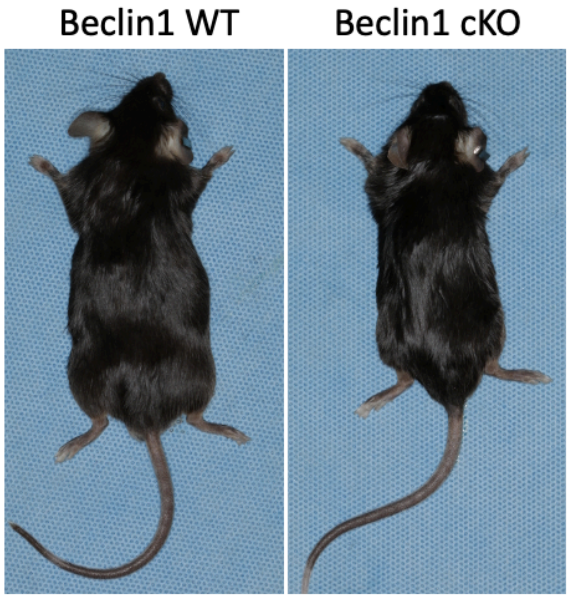

Figure 1. Photographs of 6-month-old Beclin1 WT and KO mice.

2

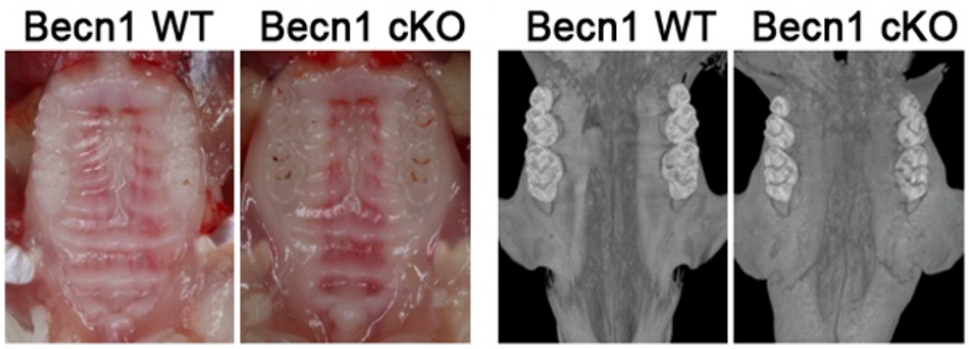

Figure 2. Oral mucosa of maxilla in 6-month-old Beclin1 WT and cKO mice. Photograph of the occlusal view of maxilla (left). μCT image of the occusal view of maxilla (right).

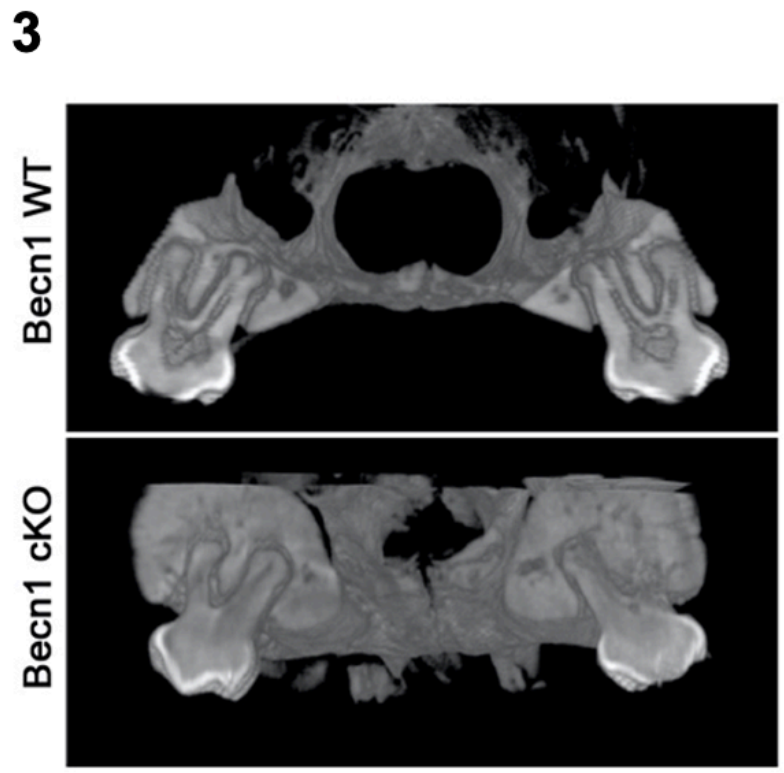

Figure 3. μCT image of sagittal cross section in 6-month-old maxilla.

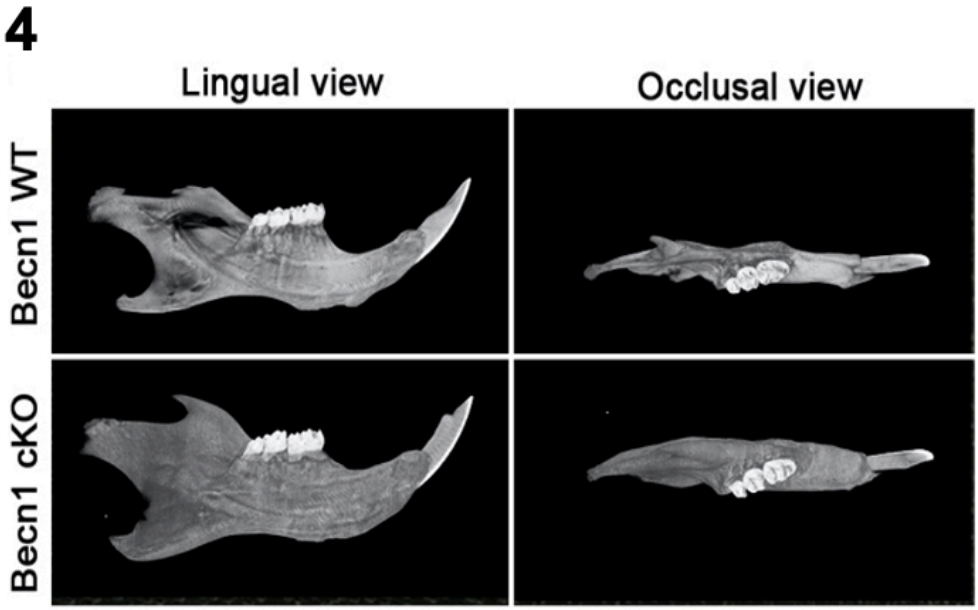

Figure 4. μCT image of mandibles in 6-month-old Beclin1 WT and cKO mice.

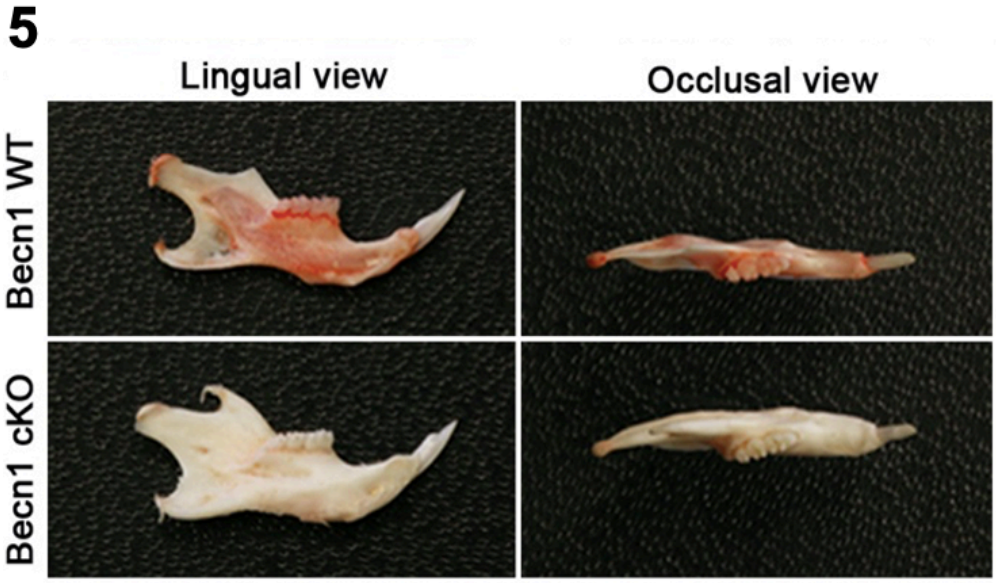

Figure 5. Photographs of mandibles from 6-month-old Beclin1 WT and cKO mice.

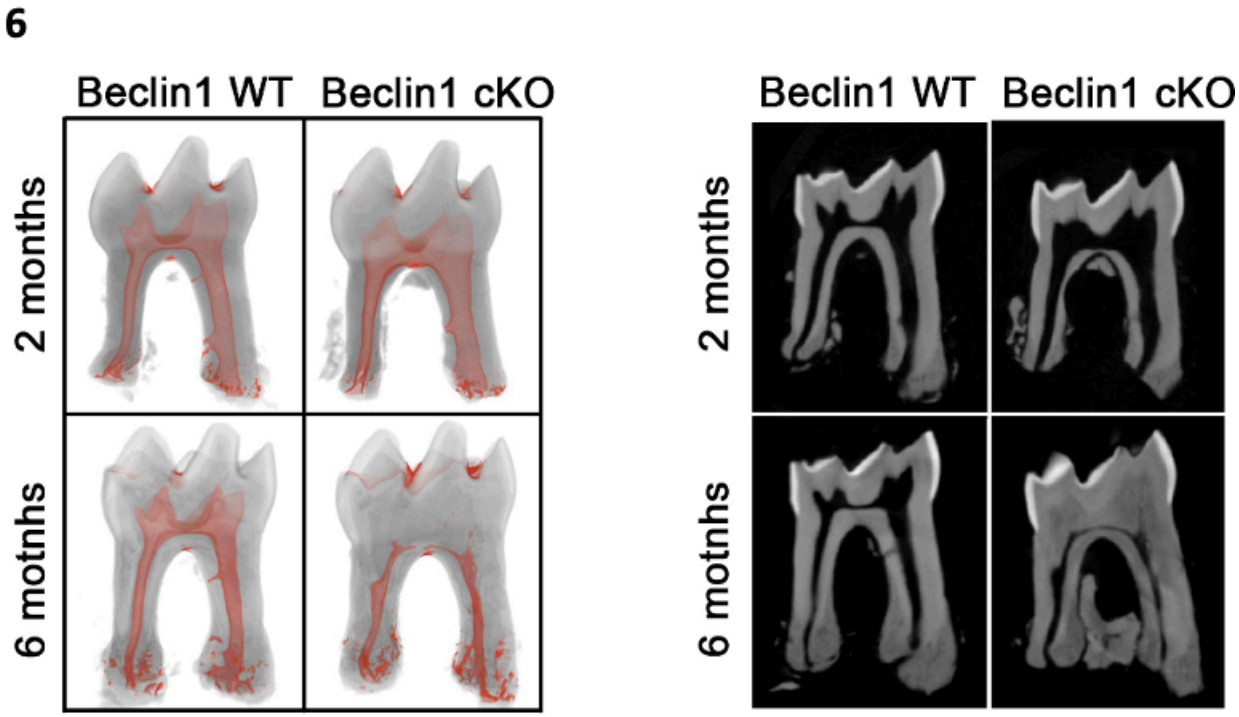

Figure 6. Molars in 2 and 6-month-old Beclin1 WT and cKO mice (N = 9 WT, N = 7 KO). Pulp chamber images with hard tissue (left). µCT image of molars (right).

7

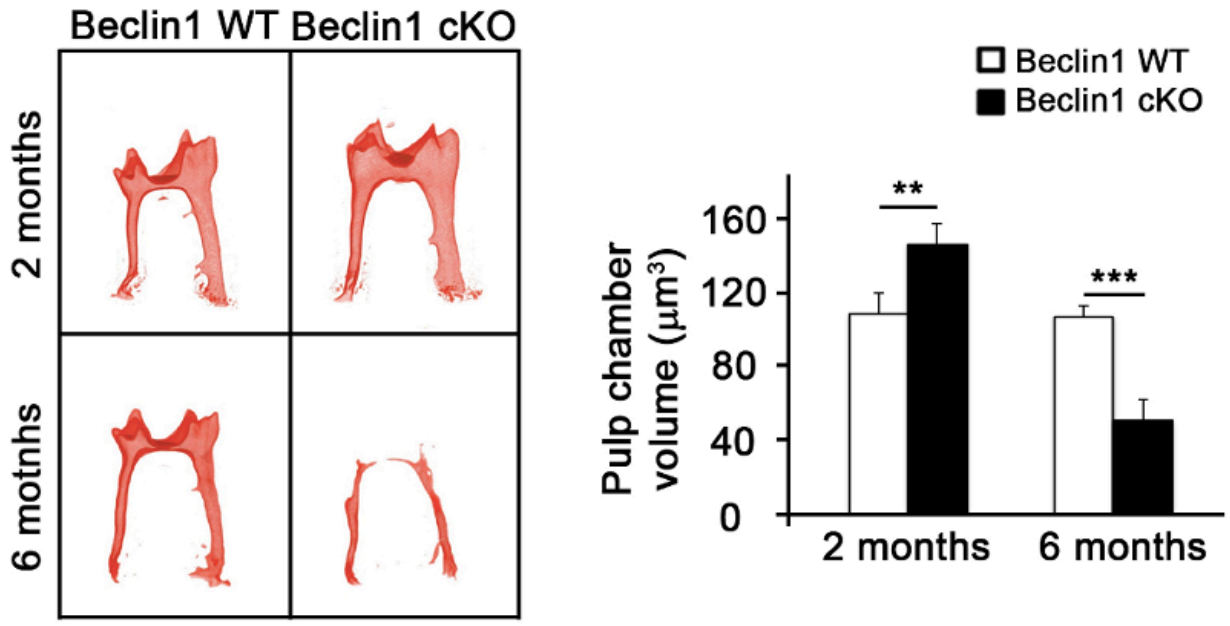

Figure 7. Pulp chamber of molars in 2 and 6-month-old Beclin1 WT and cKO mice. Pulp chamber images of 2 and 6-month-old mice (left). Quantification of pulp chamber volume in μm^3 (right).

8

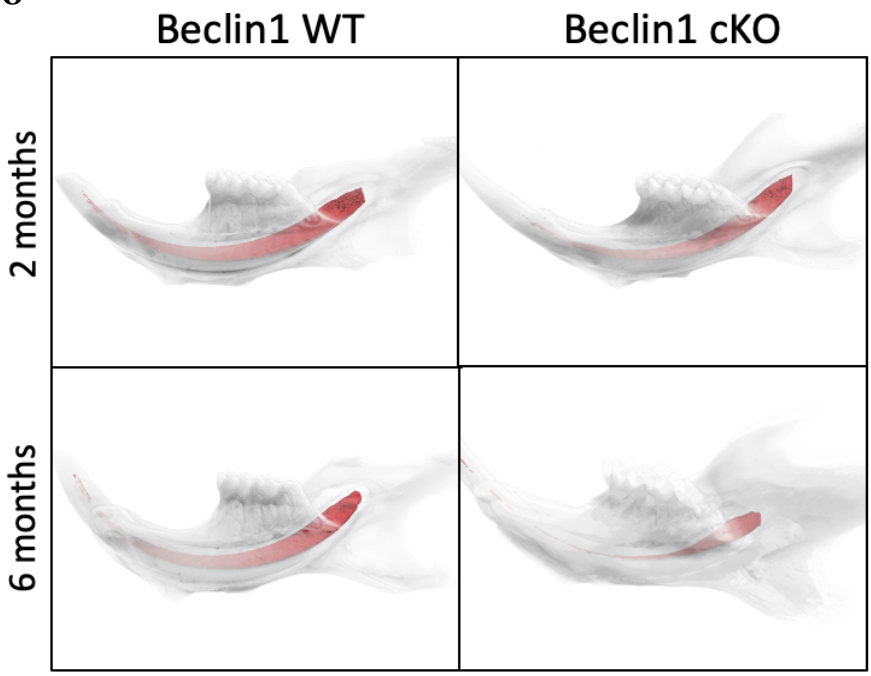

Figure 8. Incisor pulp chamber images with hard tissue in 2 and 6-month-old Beclin1 WT and cKO mice. (N = 3 WT, N = 3 KO)

9

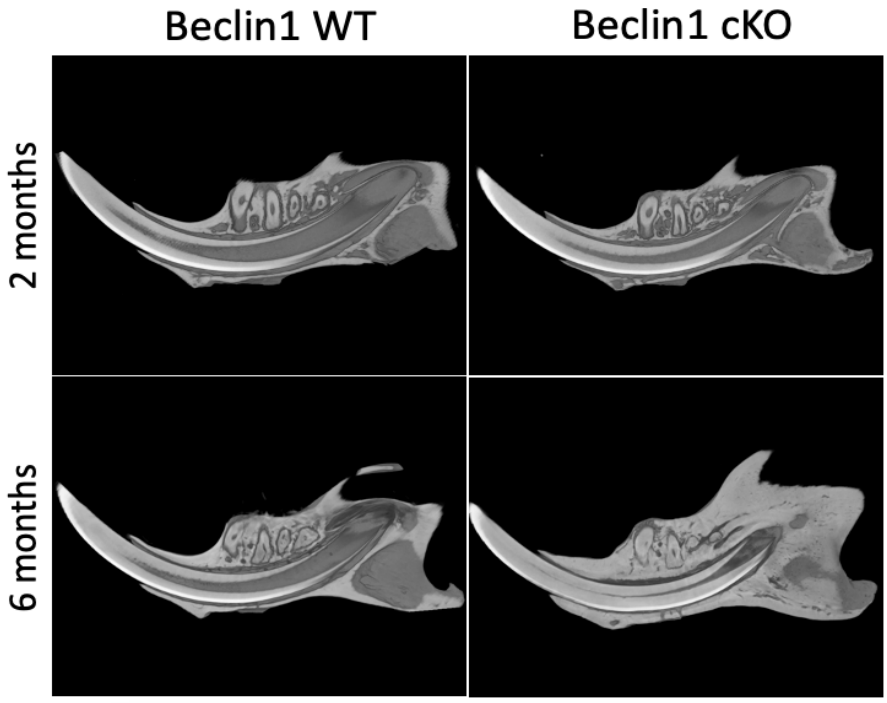

Figure 9. µCT of incisors in 2 and 6-month-old Beclin1 WT and cKO mice.

10

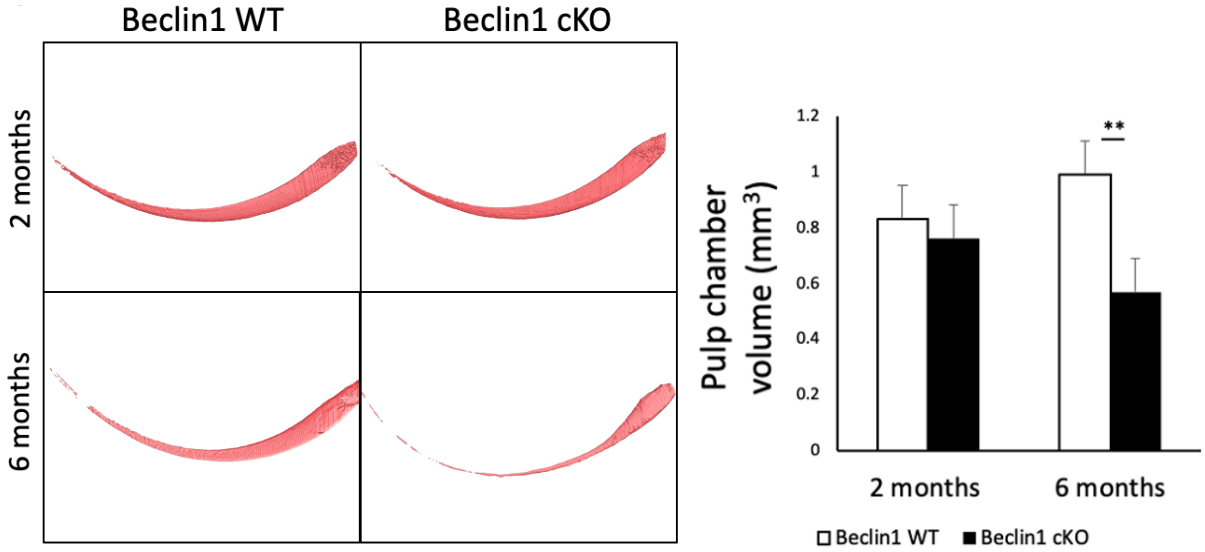

Figure 10. Pulp chamber of incisors in 2 and 6-month-old Beclin1 WT and cKO mice. Pulp chamber images (left). Quantification of pulp chamber volume in mm^3 (right).

11

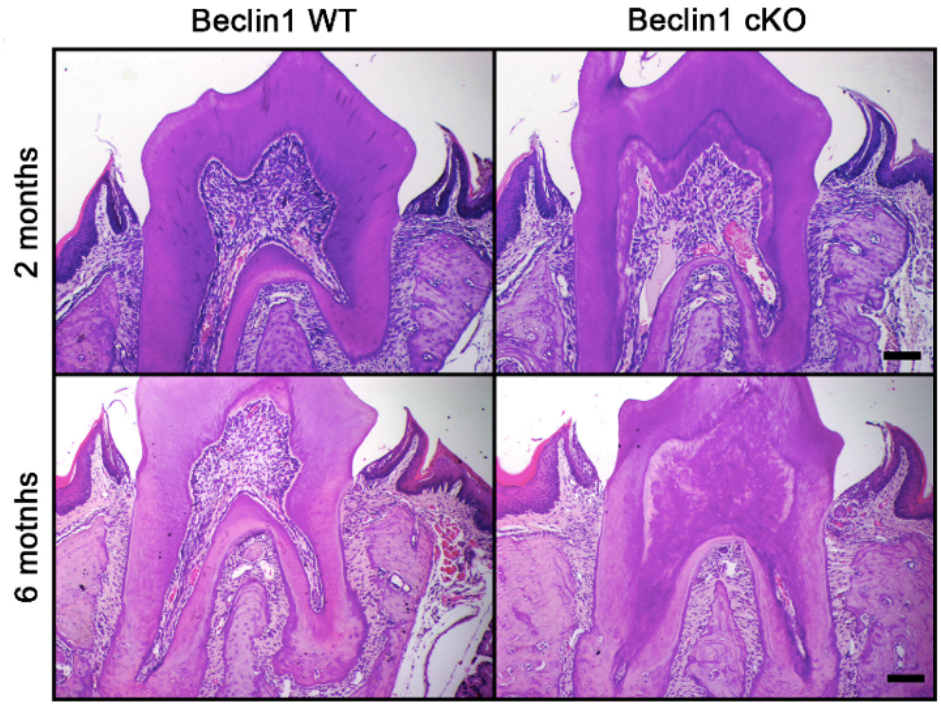

Figure 11. Histological analysis of molars in 2 and 6-month-old Beclin1 WT and cKO mice with H&E staining. Scale = 100 um.

12

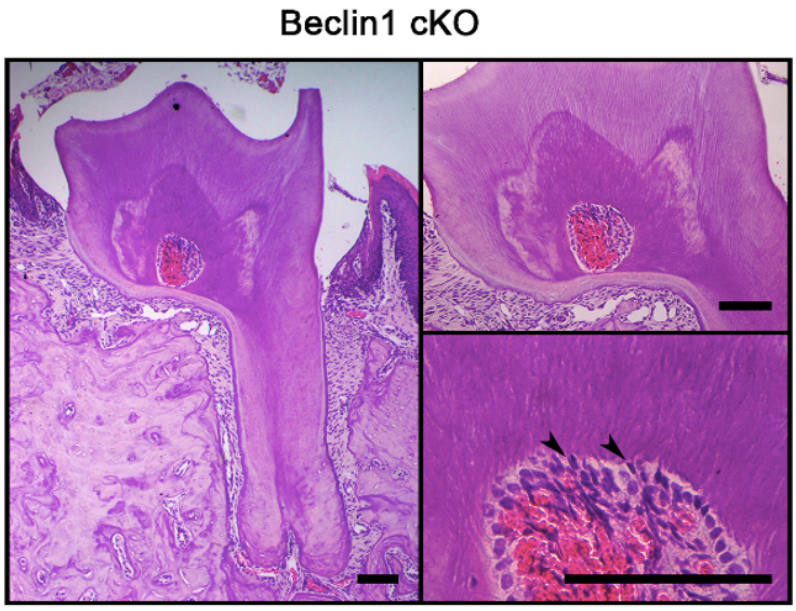

Figure 12. Histological analysis of molars in 6-month-old cKO mice exhibiting a diminishing mesenchyme. Scale = 100 um.

13

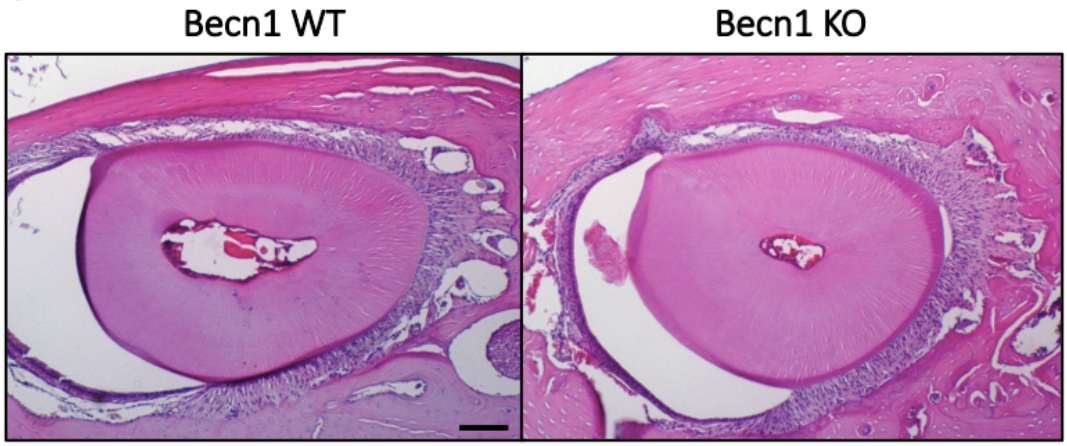

Figure 13. H&E staining of 6-month-old Beclin1 WT and KO incisors. Scale = 100 um.

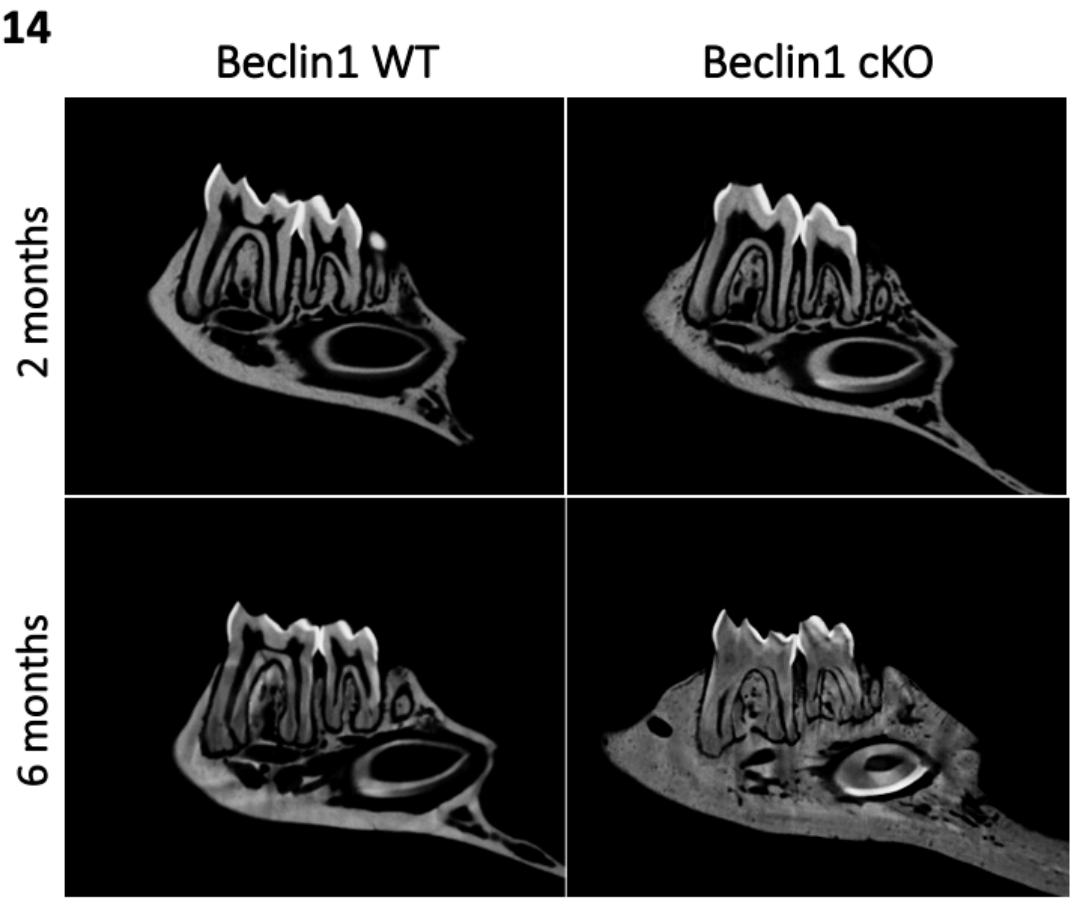

Figure 14. Diagonal cross section μCT image of 2 and 6-month-old Beclin1 WT and KO mandibles.

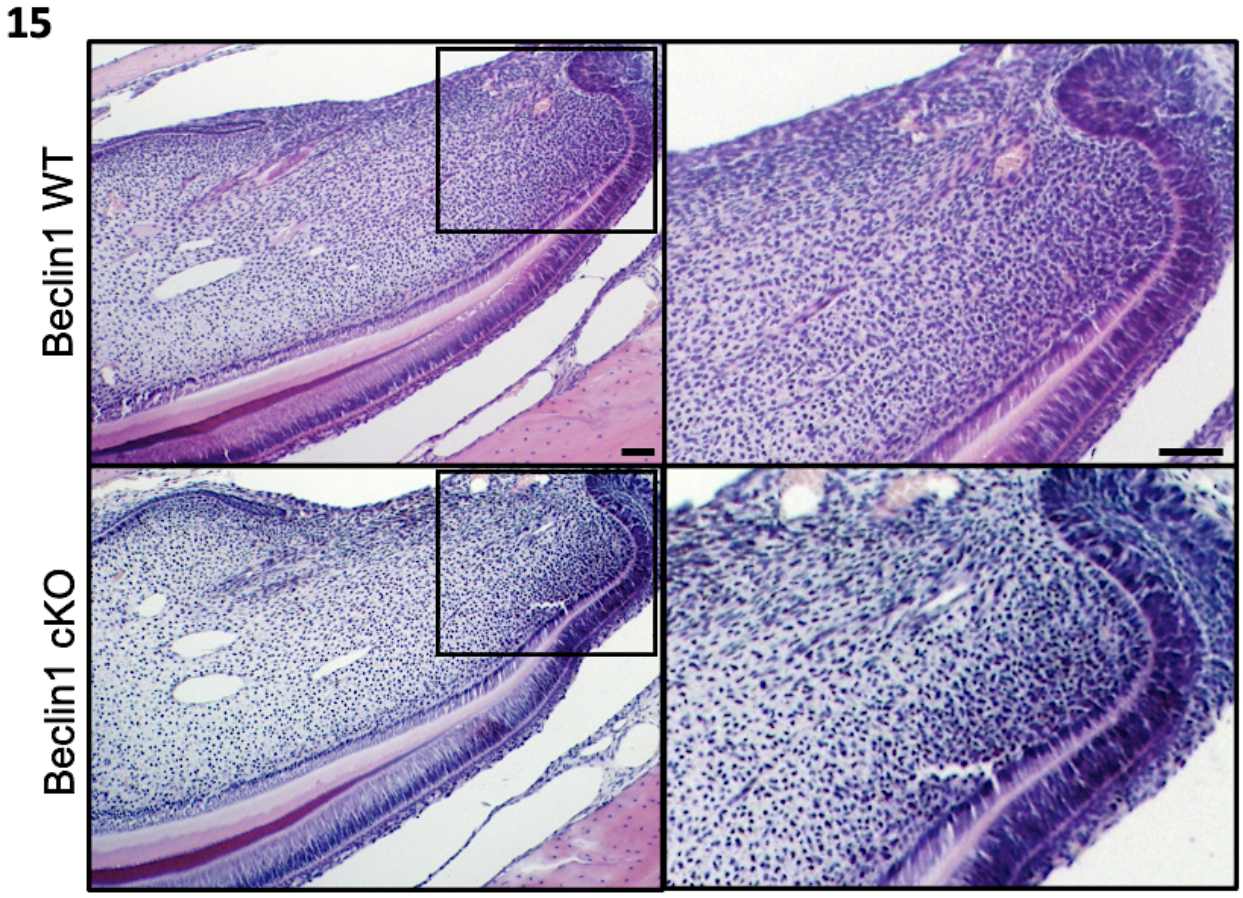

Figure 15. H&E staining of laCL in 6-month-old Beclin1 WT and cKO mice. Magnification of the boxes in the left image (right).

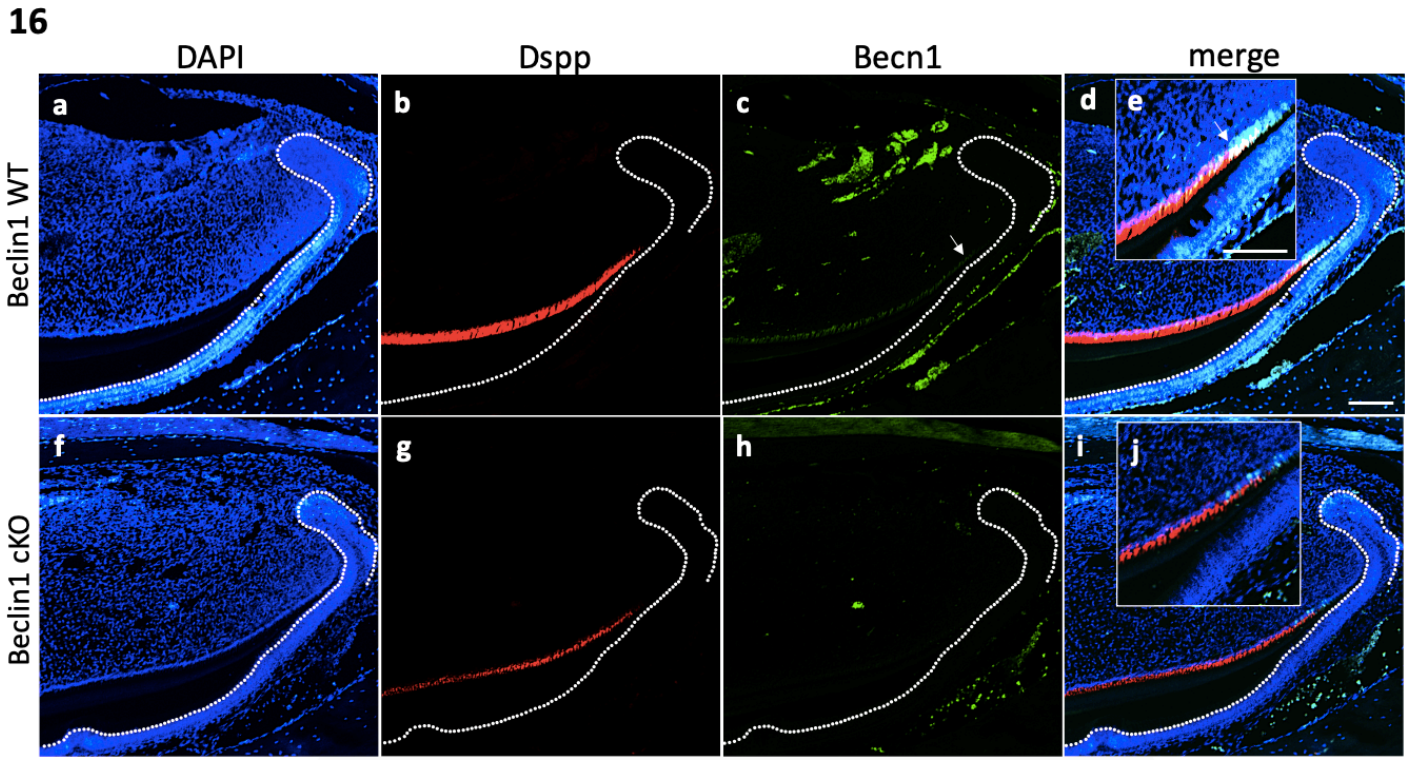

Figure 16. RNAscope *in situ hybridization* of *Dspp* and *Beclin1* in the laCL of 6-month-old mice. (A-E) Staining in Beclin1 WT mice. White arrow in Figure C points to the start of *Beclin1 mRNA* expression. White arrow in Figure E points to the start of *Dspp-Beclin1* colocalization. (F-J) Staining in Beclin1 cKO mice. (E) Magnified image of D. (J) Magnified image of I.

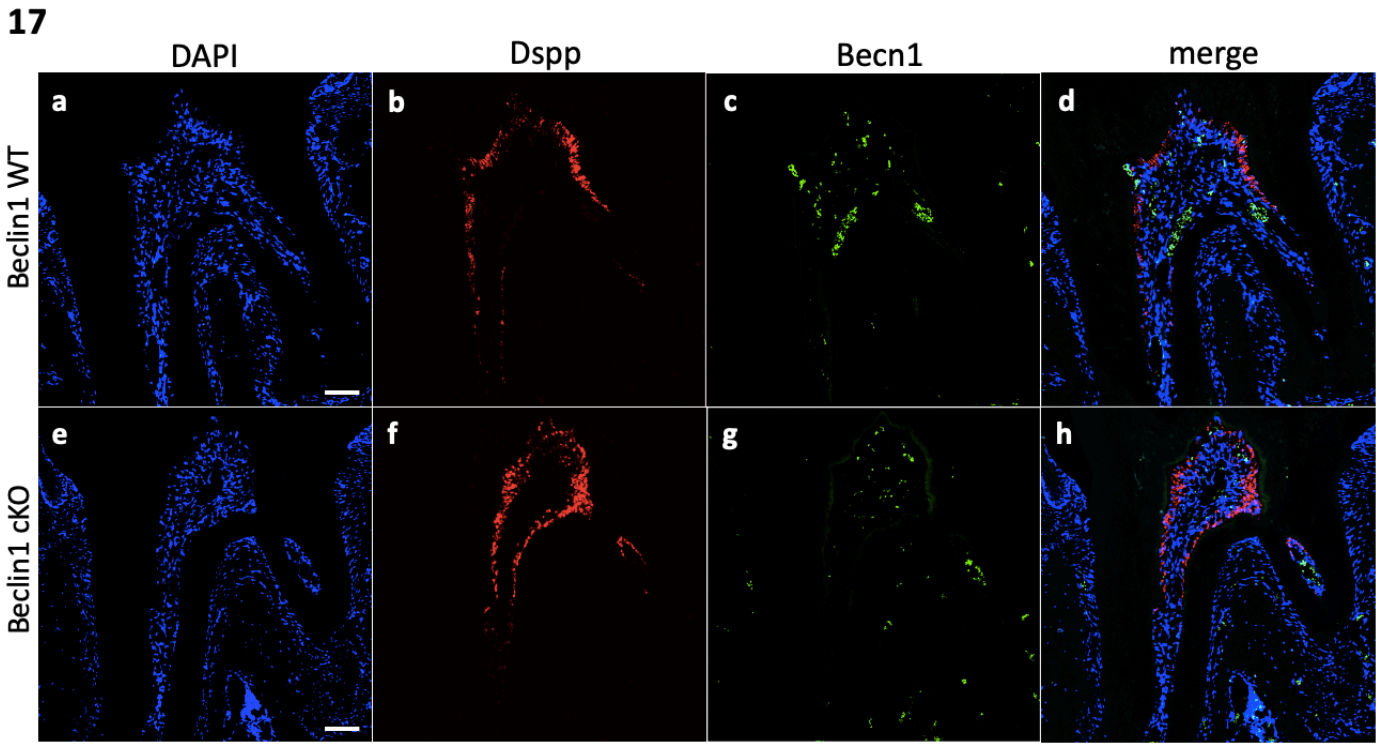

Figure 17. RNAscope *in situ hybridization* of *Dspp* and *Beclin1* in 2-month-old mice molars. (A-D). Staining of 2-month-old Beclin1 WT mice. (E-H) ISH staining of 2-month-old Beclin1 KO mice.

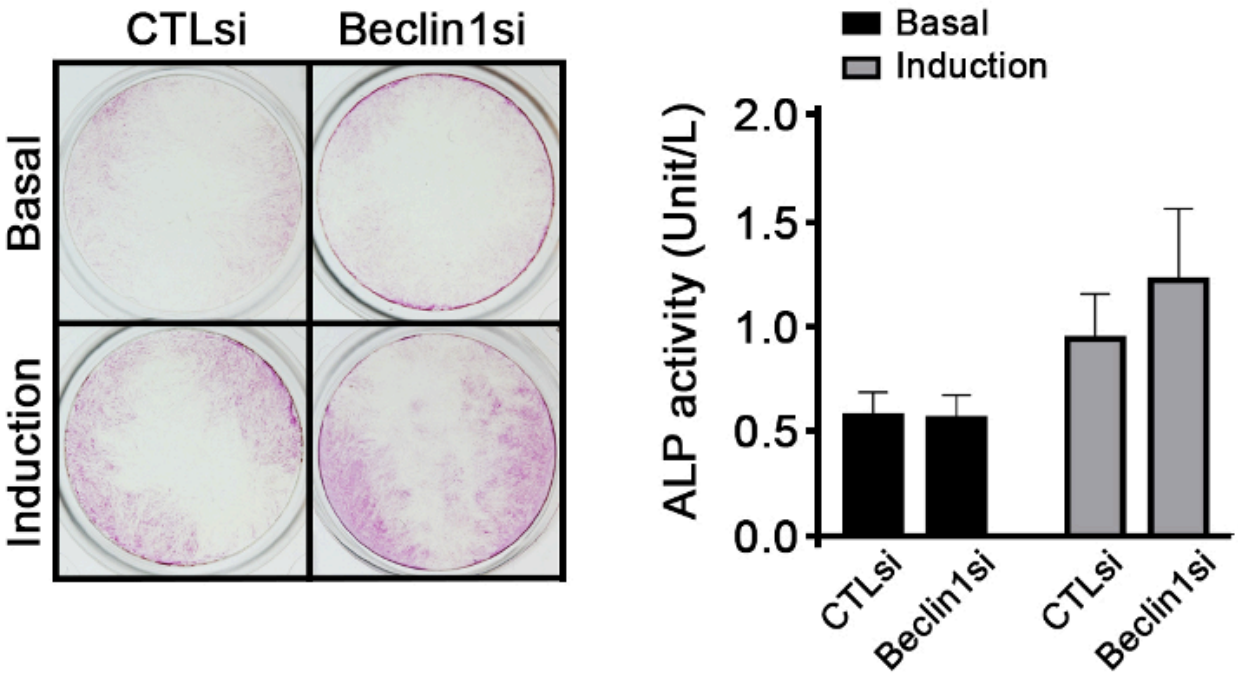

Figure 18. ALP staining of siBeclin1-treated DPSCs upon odontogenic induction.

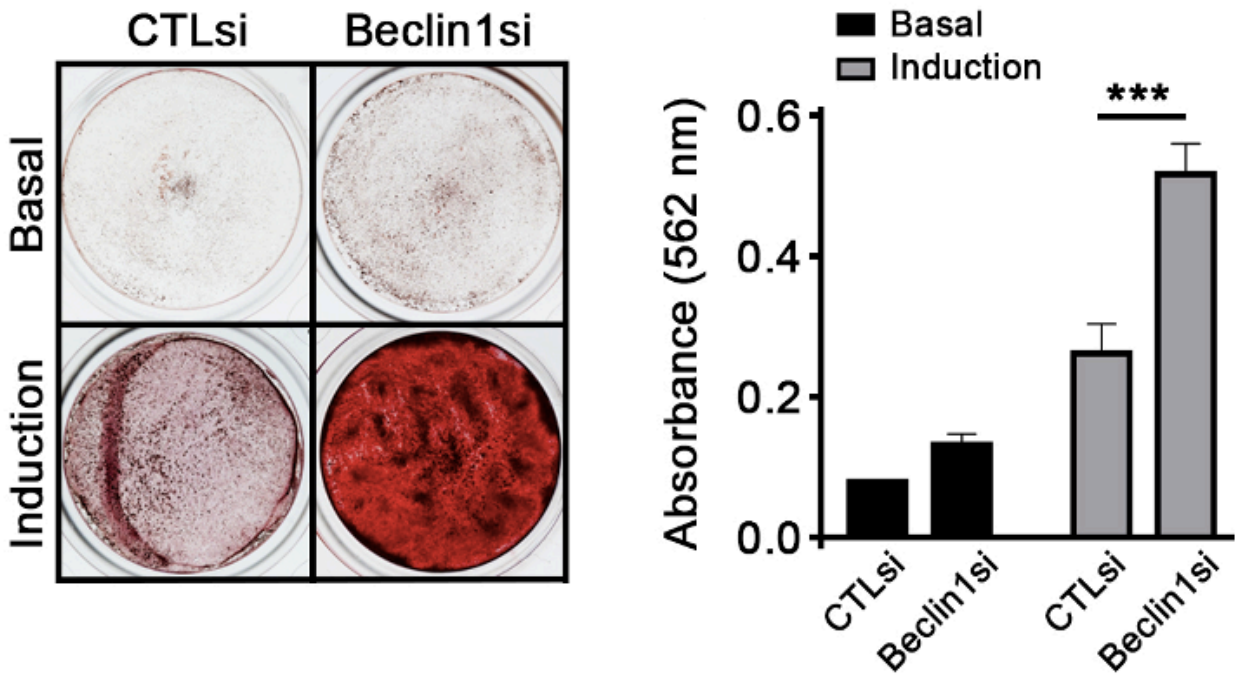

Figure 19. Alizarin Red S Staining of siBeclin1-treated DPSCs upon odontogenic induction.

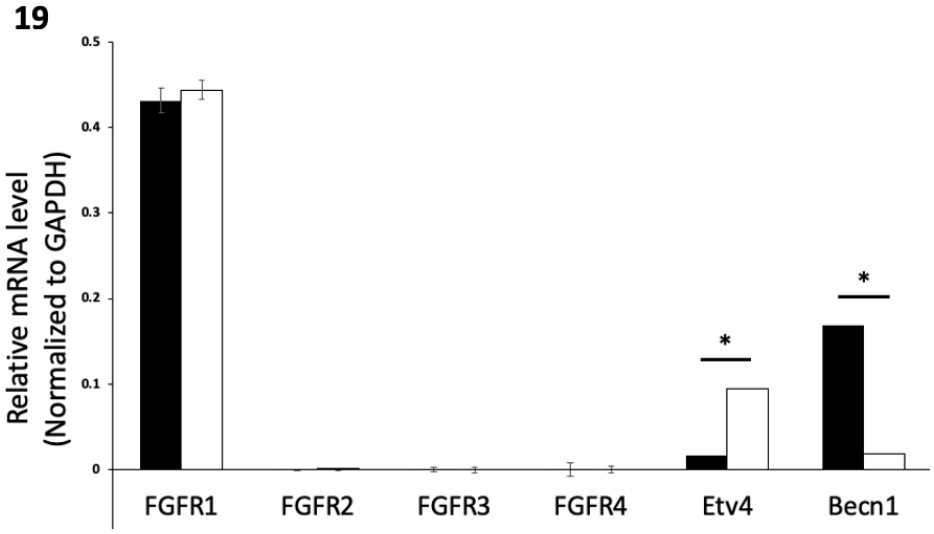

Figure 20. Relative mRNA expression level of *Fgfr1, Fgfr2, Fgfr3, Fgfr4, Etv4,* and *Beclin1*.

References

Feng, Y., He, D., Yao, Z. *et al.* The machinery of macroautophagy. *Cell Res* **24,** 24–41 (2014). https://doi.org/10.1038/cr.2013.168

Lee JM, Wagner M, Xiao R, Kim KH, Feng D, Lazar MA, Moore DD. Nutrient-sensing nuclear receptors coordinate autophagy. Nature. 2014 Dec 4;516(7529):112-5. doi: 10.1038/nature13961. Epub 2014 Nov 12. PMID: 25383539; PMCID: PMC4267857.

Kametaka,S., Okano,T., Ohsumi,M. & Ohsumi,Y. Apg14p and Apg6/Vps30p form a protein complex essential for autophagy in the yeast, *Saccharomyces cerevisiae*. *J. Biol. Chem.* **273**, 22284 –22291 (1998).

Aita,V. M. *et al*. Cloning and genomic structure of *beclin 1*, a candidate tumor suppressor gene on chromosome 17q21. *Genomics* **59**, 59–65 (1999).

Zhang L, Chen Z. Autophagy in the dentin-pulp complex against inflammation. Oral Dis. 2018 Mar;24(1-2):11-13. doi: 10.1111/odi.12749. PMID: 29480617.

Couve E, Osorio R, Schmachtenberg O. The amazing odontoblast: activity, autophagy, and aging. J Dent Res. 2013 Sep;92(9):765-72. doi: 10.1177/0022034513495874. Epub 2013 Jun 26. PMID: 23803461.

Zhan Y, Wang H, Zhang L, Pei F, Chen Z. HDAC6 Regulates the Fusion of Autophagosome and Lysosome to Involve in Odontoblast Differentiation. Front Cell Dev Biol. 2020 Nov 26;8:605609. doi: 10.3389/fcell.2020.605609. PMID: 33330506; PMCID: PMC7732691.

Lee YH, Lee HY, Kim TG, Lee NH, Yu MK, Yi HK. PPARγ Maintains Homeostasis through Autophagy Regulation in Dental Pulp. J Dent Res. 2015 May;94(5):729-37. doi: 10.1177/0022034515573833. Epub 2015 Mar 5. PMID: 25744070.

Zhang Z, Singh R, Aschner M. Methods for the Detection of Autophagy in Mammalian Cells. Curr Protoc Toxicol. 2016 Aug 1;69:20.12.1-20.12.26. doi: 10.1002/cptx.11. PMID: 27479363; PMCID: PMC4982470.

Pei F, Wang HS, Chen Z, Zhang L. Autophagy regulates odontoblast differentiation by suppressing NF-κB activation in an inflammatory environment. Cell Death Dis. 2016 Mar 3;7(3):e2122. doi: 10.1038/cddis.2015.397. PMID: 26938294; PMCID: PMC4823923.

Boya P, Reggiori F, Codogno P. Emerging regulation and functions of autophagy. Nat Cell Biol. 2013 Jul;15(7):713-20. doi: 10.1038/ncb2788. Erratum in: Nat Cell Biol. 2013 Aug;15(8):1017. PMID: 23817233; PMCID: PMC7097732.

Xing S, Zhang Y, Li J, Zhang J, Li Y, Dang C, Li C, Fan Y, Yu J, Pei Z, Zeng J. Beclin 1 knockdown inhibits autophagic activation and prevents the secondary neurodegenerative damage in the ipsilateral thalamus following focal cerebral infarction. Autophagy. 2012 Jan;8(1):63-76. doi: 10.4161/auto.8.1.18217. Epub 2012 Jan 1. PMID: 22108007.

Pattingre S, Tassa A, Qu X, Garuti R, Liang XH, Mizushima N, Packer M, Schneider MD, Levine B. Bcl-2 antiapoptotic proteins inhibit Beclin 1-dependent autophagy. Cell. 2005 Sep 23;122(6):927-39. doi: 10.1016/j.cell.2005.07.002. PMID: 16179260.

Wei Y, Pattingre S, Sinha S, Bassik M, Levine B. JNK1-mediated phosphorylation of Bcl-2 regulates starvation-induced autophagy. Mol Cell. 2008 Jun 20;30(6):678-88. doi: 10.1016/j.molcel.2008.06.001. PMID: 18570871; PMCID: PMC2478643.

Arai A, Kim S, Goldshteyn V, Kim T, Park NH, Wang CY, Kim RH. Beclin1 Modulates Bone Homeostasis by Regulating Osteoclast and Chondrocyte Differentiation. J Bone Miner Res. 2019 Sep;34(9):1753-1766. doi: 10.1002/jbmr.3756. Epub 2019 Jul 30. PMID: 31074883.

A. Ohazama, J. Blackburn, T. Porntaveetus, M.S. Ota, H.Y. Choi, E.B. Johnson, P. Myers, S. Oommen, K. Eto, J.A. Kessler, T. Kondo, G.J. Fraser, J.T. Streelman, U.F.J. Pardiñas, A.S. Tucker, P.E. Ortiz, C. Charles, L. Viriot, J. Herz, P.T. Sharpe. A role for suppressed incisor cuspal morphogenesis in the evolution of mammalian heterodont dentition Proc. Nat. Acad. Sci. USA, 107 (2010), pp. 92-97

Yu T, Klein OD. Molecular and cellular mechanisms of tooth development, homeostasis and repair. Development. 2020 Jan 24;147(2):dev184754. doi: 10.1242/dev.184754. PMID: 31980484; PMCID: PMC6983727.

Kaukua N, Shahidi MK, Konstantinidou C, Dyachuk V, Kaucka M, Furlan A, An Z, Wang L, Hultman I, Ahrlund-Richter L, Blom H, Brismar H, Lopes NA, Pachnis V, Suter U, Clevers H, Thesleff I, Sharpe P, Ernfors P, Fried K, Adameyko I. Glial origin of mesenchymal stem cells in a tooth model system. Nature. 2014 Sep 25;513(7519):551-4. doi: 10.1038/nature13536. Epub 2014 Jul 27. PMID: 25079316.

Zhang YD, Chen Z, Song YQ, Liu C, Chen YP. Making a tooth: growth factors, transcription factors, and stem cells. Cell Res. 2005 May;15(5):301-16. doi: 10.1038/sj.cr.7290299. PMID: 15916718.

Gibson MP, Zhu Q, Wang S, Liu Q, Liu Y, Wang X, Yuan B, Ruest LB, Feng JQ, D'Souza RN, Qin C, Lu Y. The rescue of dentin matrix protein 1 (DMP1)-deficient tooth defects by the transgenic expression of dentin sialophosphoprotein (DSPP) indicates that DSPP is a downstream effector molecule of DMP1 in dentinogenesis. J Biol Chem. 2013 Mar 8;288(10):7204-14. doi: 10.1074/jbc.M112.445775. Epub 2013 Jan 24. PMID: 23349460; PMCID: PMC3591629.

Narayanan K, Gajjeraman S, Ramachandran A, Hao J, George A. Dentin matrix protein 1 regulates dentin sialophosphoprotein gene transcription during early odontoblast differentiation. J Biol Chem. 2006 Jul 14;281(28):19064-71. doi: 10.1074/jbc.M600714200. Epub 2006 May 5. PMID: 16679514.

Chang B, Svoboda KKH, Liu X. Cell polarization: From epithelial cells to odontoblasts. Eur J Cell Biol. 2019 Jan;98(1):1-11. doi: 10.1016/j.ejcb.2018.11.003. Epub 2018 Nov 17. PMID: 30473389; PMCID: PMC6338482

Ruch JV, Lesot H, Bègue-Kirn C. Odontoblast differentiation. Int J Dev Biol. 1995 Feb;39(1):51-68. PMID: 7626422.

Prasad M, Butler WT, Qin C. Dentin sialophosphoprotein in biomineralization. Connect Tissue Res. 2010 Oct;51(5):404-17. doi: 10.3109/03008200903329789. PMID: 20367116; PMCID: PMC2933432.

Ornitz DM, Itoh N. Fibroblast growth factors. Genome Biol. 2001;2(3):REVIEWS3005. doi: 10.1186/gb-2001-2-3-reviews3005. Epub 2001 Mar 9. PMID: 11276432; PMCID: PMC138918.

Itoh N, Ornitz DM. Evolution of the Fgf and Fgfr gene families. Trends Genet. 2004 Nov;20(11):563-9. doi: 10.1016/j.tig.2004.08.007. PMID: 15475116

Ornitz DM, Marie PJ. Fibroblast growth factor signaling in skeletal development and disease. Genes Dev. 2015 Jul 15;29(14):1463-86. doi: 10.1101/gad.266551.115. PMID: 26220993; PMCID: PMC4526732.

Li CY, Prochazka J, Goodwin AF, Klein OD. Fibroblast growth factor signaling in mammalian tooth development. Odontology. 2014 Jan;102(1):1-13. doi: 10.1007/s10266-013-0142-1. Epub 2013 Dec 17. PMID: 24343791.

Li CY, Cha W, Luder HU, Charles RP, McMahon M, Mitsiadis TA, Klein OD. E-cadherin regulates the behavior and fate of epithelial stem cells and their progeny in the mouse incisor. Dev Biol. 2012 Jun 15;366(2):357-66. doi: 10.1016/j.ydbio.2012.03.012. Epub 2012 Apr 18. PMID: 22537490; PMCID: PMC3690274.

Reitsma JH, Ongkosuwito EM, van Wijk AJ, Prahl-Andersen B. Patterns of tooth agenesis in patients with crouzon or apert syndrome. Cleft Palate Craniofac J. 2014 Mar;51(2):178-83. doi: 10.1597/12-180. Epub 2012 Nov 5. PMID: 23126314.

Shi C, Yuan Y, Guo Y, Jing J, Ho TV, Han X, Li J, Feng J, Chai Y. BMP Signaling in Regulating Mesenchymal Stem Cells in Incisor Homeostasis. J Dent Res. 2019 Jul;98(8):904-911. doi: 10.1177/0022034519850812. Epub 2019 May 28. PMID: 31136721; PMCID: PMC6616121.

McKenzie J, Smith C, Karuppaiah K, Langberg J, Silva MJ, Ornitz DM. Osteocyte Death and Bone Overgrowth in Mice Lacking Fibroblast Growth Factor Receptors 1 and 2 in Mature Osteoblasts and Osteocytes. J Bone Miner Res. 2019 Sep;34(9):1660-1675. doi: 10.1002/jbmr.3742. Epub 2019 Jun 17. PMID: 31206783; PMCID: PMC6744314.

Cinque L, Forrester A, Bartolomeo R, Svelto M, Venditti R, Montefusco S, Polishchuk E, Nusco E, Rossi A, Medina DL, Polishchuk R, De Matteis MA, Settembre C. FGF signalling regulates bone growth through autophagy. Nature. 2015 Dec 10;528(7581):272-5. doi: 10.1038/nature16063. Epub 2015 Nov 23. PMID: 26595272.

Sahani MH, Itakura E, Mizushima N. Expression of the autophagy substrate SQSTM1/p62 is restored during prolonged starvation depending on transcriptional upregulation and autophagy-derived amino acids. Autophagy. 2014 Mar;10(3):431-41. doi: 10.4161/auto.27344. Epub 2014 Jan 3. PMID: 24394643; PMCID: PMC4077882.

Diez Del Corral R, Morales AV. The Multiple Roles of FGF Signaling in the Developing Spinal Cord. Front Cell Dev Biol. 2017 Jun 2;5:58. doi: 10.3389/fcell.2017.00058. PMID: 28626748; PMCID: PMC5454045.

Cotzomi-Ortega I, Aguilar-Alonso P, Reyes-Leyva J, Maycotte P. Autophagy and Its Role in Protein Secretion: Implications for Cancer Therapy. Mediators Inflamm. 2018 Dec 6;2018:4231591. doi: 10.1155/2018/4231591. PMID: 30622432; PMCID: PMC6304875.

Tanida I, Ueno T, Kominami E. LC3 and Autophagy. Methods Mol Biol. 2008;445:77-88. doi: 10.1007/978-1-59745-157-4_4. PMID: 18425443.

Couve E, Schmachtenberg O. Autophagic activity and aging in human odontoblasts. J Dent Res. 2011 Apr;90(4):523-8. doi: 10.1177/0022034510393347. Epub 2011 Jan 6. PMID: 21212314.

Krivanek J, Soldatov RA, Kastriti ME, Chontorotzea T, Herdina AN, Petersen J, Szarowska B, Landova M, Matejova VK, Holla LI, Kuchler U, Zdrilic IV, Vijaykumar A, Balic A, Marangoni P, Klein OD, Neves VCM, Yianni V, Sharpe PT, Harkany T, Metscher BD, Bajénoff M, Mina M, Fried K, Kharchenko PV, Adameyko I. Dental cell type atlas reveals stem and differentiated cell types in mouse and human teeth. Nat Commun. 2020 Sep 23;11(1):4816. doi: 10.1038/s41467-020-18512-7. PMID: 32968047; PMCID: PMC7511944.